Numerical studies on convection in GTA Weld Pool

P. Maran[1] T. Sornakumar[2] and T. Sundararajan[3]
[1]Department of Mechanical Engineering, Thiagarajar College of Engineering, Madurai
[2]Department of Mechanical Engineering, Thiagarajar College of Engineering, Madurai
[3]Department of Mechanical Engineering, Indian Institute of Technology, Madras, Chennai

ABSTRACT

Weld pool convection strongly influences the behaviour of molten metal in the melt pool during fusion welding of metals. The temperature and velocity fields in the melt pool are largely affected by different driving forces causing weld pool convection. Variations in the heat input during welding have significant effects on the peak temperature, maximum velocity in the melt pool and weld bead geometry. Buoyancy, electromagnetic and surface tension are the major driving forces. In the present work, the effects of weld pool convection on weld bead geometry of stainless steel during Gas Tungsten Arc (GTA) welding have been studied for individual and combined driving forces. A two dimensional finite volume model has been used to simulate the welding process. The model uses a modified Gaussian heat distribution to provide the three dimensional effect of linear welding.

Keywords : Modeling, weld pool, fluid flow, GTA welding, stainless steel, weld bead geometry.

Nomenclature

T - temperature, K,

T_{ref} reference temperature, K,

p pressure, Nm^{-2}

C_p - specific heat, $Jm^{-3}K^{-1}$.

t - time, second,

g - acceleration due to gravity, ms^{-2},

J_x current density in x direction, Am^{-2},

J_y current density in y direction, Am^{-2},

k - thermal conductivity, $Wm^{-1}K^{-1}$,

u - velocity in x direction, ms^{-1},

v - velocity in y direction, ms^{-1}

x distance in x direction, m,

y distance in y direction, m/s,

μ dynamic viscosity, kg m /s

ρ density, kg/m^3

- thermal expansion coefficient, K^{-1} and

B_θ azimuthal magnetic field, Wbm^{-2}

INTRODUCTION

Fusion welding develops a molten pool just below the welding torch and the weldment is formed immediately after the solidification. Even though the time required for solidification is less than a second, the liquid metal in the pool has movement within the weld pool and strongly influences the weld pool geometry. The fluid flow pattern is largely affected by the different forces that are acting on the weld pool. The major driving forces are buoyancy, electromagnetic and surface tension forces. The prediction of the effect of these forces and proper control over the welding process parameters will help us to get weld bead with better aspect ratio and quality.

The development of numerical models began in the 1940s with analytical solutions by Rosenthal [1] but it grew rapidly during the 1980s with the onset of powerful computers. Heat and fluid flow models [2-4] were developed to study the effect of weld pool convection on weld bead geometry, considering individual and combined driving forces. Investigations were also made to understand the effect of deformed free surface and arc pressure [5-7]. Fan et al. [8] developed a computational model of stationary gas tungsten arc weld pools and compared the results with experimental results. Three dimensional heat and fluid flow models [4,9,10] were also developed to study the weld pool behaviour during linear welding. It was observed that the surface depression in excess of 0.1 mm is found for currents larger than 240 A. The effect of arc pressure on penetration is very little at 100 A, as the free surface deformation is less than 0.02 mm and it is relatively high at 200 A. In the present work, a two dimensional heat and fluid flow model based on finite volume method has been

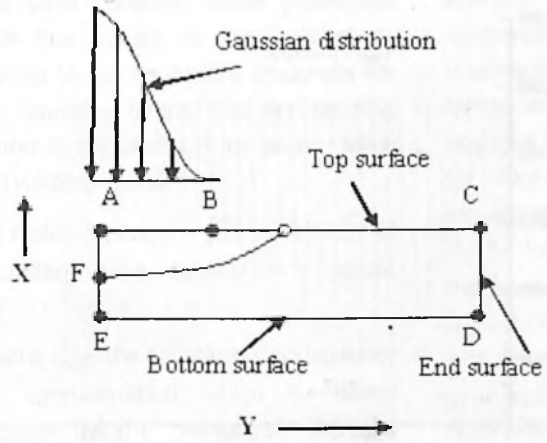

Fig 1 : Boundary conditions

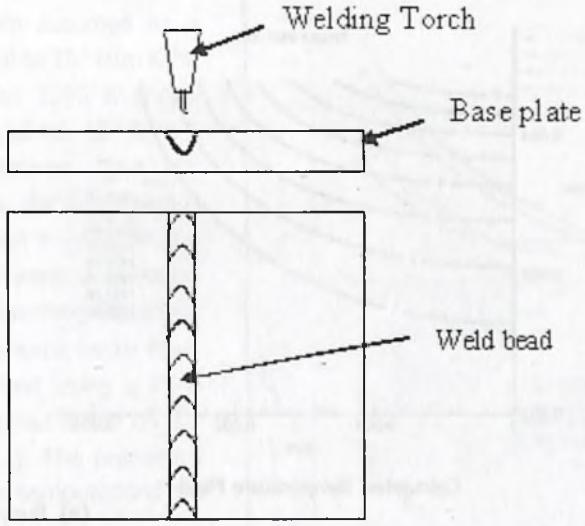

Fig 2 : Bead on plate welding

developed to study the effect of weld pool convection during linear GTA welding of stainless steel. A modified Gaussian distribution is used to provide the three dimensional effect of linear welding. The arc residing period at each cell of the computational domain is calculated from the welding speed and length of the cell in the third dimension.

MATHEMATICAL MODEL

In the present work, a heat and fluid flow model has been developed with the following assumptions:

1. A Gaussian heat distribution and current distribution.
2. Flow is Newtonian, laminar and incompressible,
3. All physical properties are constant and independent of temperature, except for thermal conductivity (k) and surface tension (γ) and
4. The free surface of the weld pool is taken to be undeformed.

The governing equations for a two dimensional heat and fluid flow problem are as follows.

continuity:

$$\frac{\partial u}{\partial x}+\frac{\partial v}{\partial y}=0 \tag{1}$$

x-momentum:

$$\rho\left(\frac{\partial u}{\partial t}+u\frac{\partial u}{\partial x}+v\frac{\partial u}{\partial y}\right)=-\frac{\partial p}{\partial x}+\mu\left(\frac{\partial^2 u}{\partial x^2}+\frac{\partial^2 u}{\partial y^2}\right)+\rho g_x\beta\left(T-T_{ref}\right)-J_y B_0 \tag{2}$$

y-momentum:

$$\rho\left(\frac{\partial v}{\partial t}+u\frac{\partial v}{\partial x}+v\frac{\partial v}{\partial y}\right)=-\frac{\partial p}{\partial y}+\mu\left(\frac{\partial^2 v}{\partial x^2}+\frac{\partial^2 v}{\partial y^2}\right)+\rho g_y\beta\left(T-T_{ref}\right)+J_x B_0 \tag{3}$$

energy:

$$\rho c_p\left(\frac{\partial T}{\partial t}+u\frac{\partial T}{\partial x}+v\frac{\partial T}{\partial y}\right)=k\left(\frac{\partial^2 T}{\partial x^2}+\frac{\partial^2 T}{\partial y^2}\right) \tag{4}$$

The boundary conditions are prescribed as shown in Figure 1. The top, side and bottom surfaces of the plate are exposed to ambient conditions during welding. Heat transfer to the surroundings occurs both by convection and radiation. The details are given in many literatures [7,8]. In general, in the solid region (with temperature less than the solidus temperature) both velocity components u and v are set to zero at all locations. The release or absorption of latent heat due to phase change at the liquid-solid interface has been considered by accounting for the latent heat in the form of an equivalent enhanced specific heat for the nodes in the phase change region (with temperature between solidus and liquidus temperatures). The computation has been carried out for the period of arcing duration at each cell, with a time step of 0.0002 s. The heat flux has a maximum value at the center of the arc and decreases along the radial direction. In the present work, the heat flux variation in the lateral (x) direction has been considered as a Gaussian profile, but it has been averaged into an

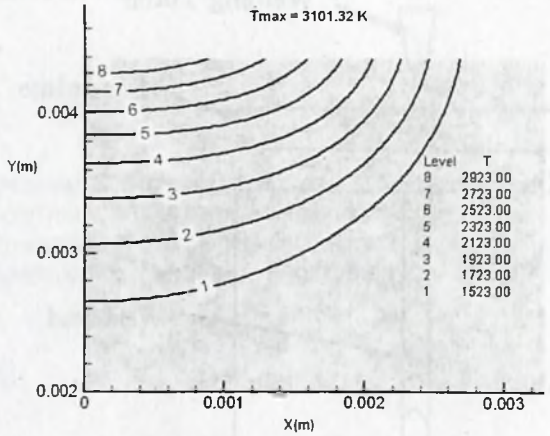

Calculated Temperature Field

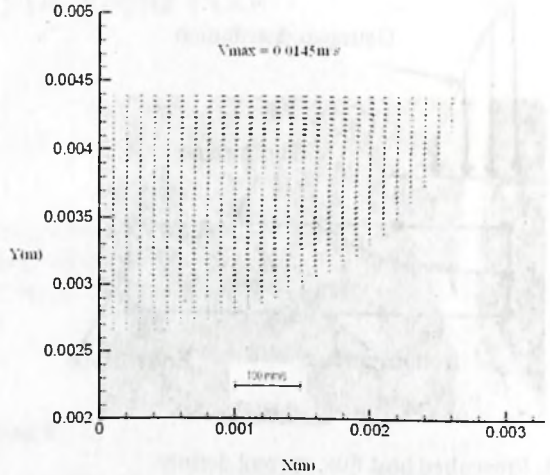

Calculated Velocity Field

(a) Buoyancy force only

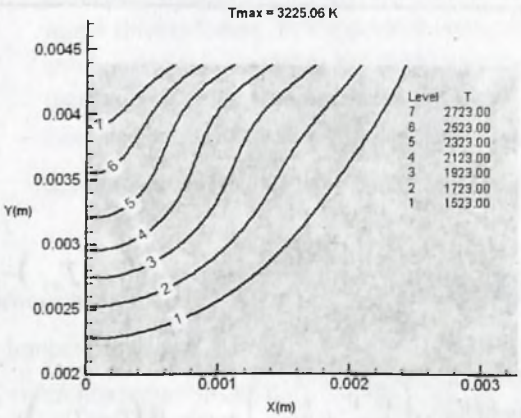

Calculated Temperature Field

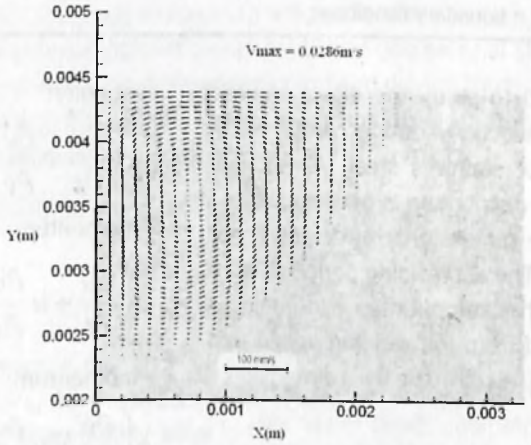

Calculated Velocity Field

(b) Electromagnetic force only

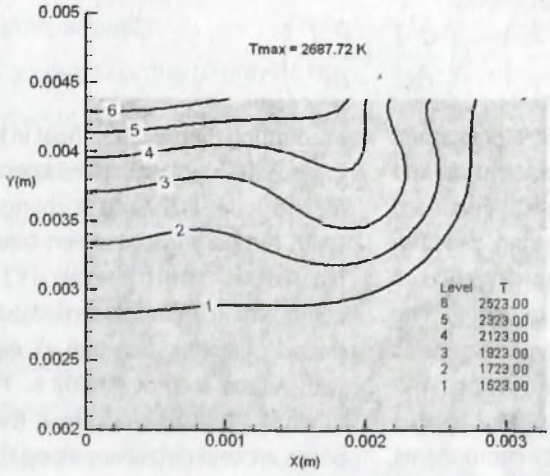

Calculated Temperature Field

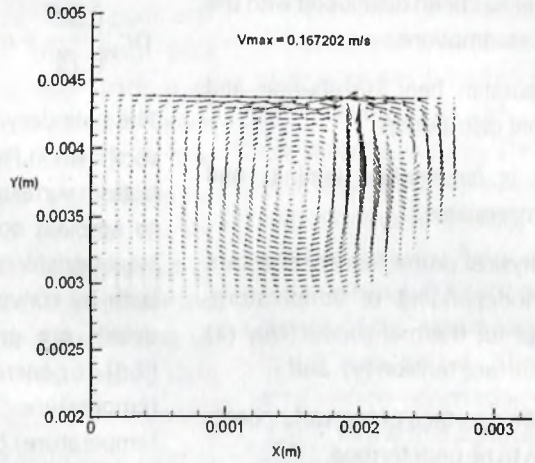

Calculated Velocity Field

(c) Surface tension force only

Fig. 3 : Effect of individual driving forces during welding at 120 A at 2.66 mm/s

equivalent constant value (maximum heat flux value) in the z-direction, leading to an equivalent thickness for the Gaussian beam. The arc residing period is calculated from beam radius and welding speed.

Arc residing period = (C_{eq} x Diameter of Gaussian base circle)/Torch speed (5)

Where, C_{eq} is the constant of equivalence for approximation which is mainly decided by the nature of Gaussian profile and in the present study and it is taken as 0.6.

Bead on plate GTA welding is made on a stainless steel plate of type AISI 304L, as shown in Figure 2. The size of the plate is 80 mm x 80 mm x 4.35 mm. One half of the plate is considered as the computational domain due to the symmetry of the plate being welded. The computational domain, a rectangle of size 40 mm x 4.35 mm, is divided into a number of rectangular cells of variable spacing. Finer grids are used nearer to the heat source, whilst further away a relatively coarser grid is employed. The mathematical model has employed an overall 80 x 80 non-uniform fixed rectangular grid system for the calculation of the temperature and velocity fields in the x-y plane. The minimum size of grid in the x direction is 0.1 mm and minimum size of grid in the y direction is 0.04 mm. For the numerical solution of governing equations, the problem domain is covered by a set of rectangular control volumes. The discretization is performed using a staggered grid that consists of temperature/velocity nodes and pressure nodes, as discussed by Raghavan et al. [11].

The individual and combined effects of driving forces on the temperature and velocity distribution in the weld pool have been studied. The gradient of surface tension with respect to temperature has been assumed as a positive constant equal to 10^{-5} N/m K for temperature less than 2200 K and a negative constant equal to 10^{-5} N/m K for higher temperatures. The arc efficiency (η) is 80 %, the beam radius (r_b) for heat distribution is 0.003 m and the beam radius for current distribution (r_i) is 0.003 m. The governing equations with the associated source terms have been numerically solved using a C++ code has been developed based on the SIMPLE algorithm [12]. The properties of material used in the computations are given in Table 1.

EXPERIMENTAL WORK

Autogenous bead-on-plate GTA welds have been made on 4.35 mm thick, AISI type 304L stainless steel plates at different electrode speeds and welding currents. The AISI type 304L stainless steel has 80 ppm sulphur content. The work material has been cut into test pieces of 80 x 80 x 4.35 mm size. Weld beads have been laid along the center line of the plate. During welding operations, the arc gap is maintained at 2 mm and the shielding gas is supplied at 16 liters per minute. The top and side surfaces have been exposed to an ambient temperature of 303 K (T_{ref}). Welding current and voltage have been measured using a digital ammeter and voltmeter, provided in the welding machine. The time taken for welding has been measured with a digital stop clock. The welded plates have been cut across the weld bead. Test specimens have been machined, polished with different grades of emery sheets and then etched to get a macroscopic view of the weld bead. The weld bead depth and width have been measured with a micrometer attached with optical microscope.

RESULTS AND DISCUSSION

The detailed information on the temperature and velocity fields in the weld pool that occur during the GTAW process is numerically obtained by solving the governing equations and the results are presented in Table 2. The effects of individual and combined driving forces have been studied for the welding condition of 120 A, 14 V and welding speed 2.66 mm/s. Figure 3 shows the calculated temperature and velocity fields for individual driving forces for the welding condition of 120 A and 14 V at a welding speed of 2.66

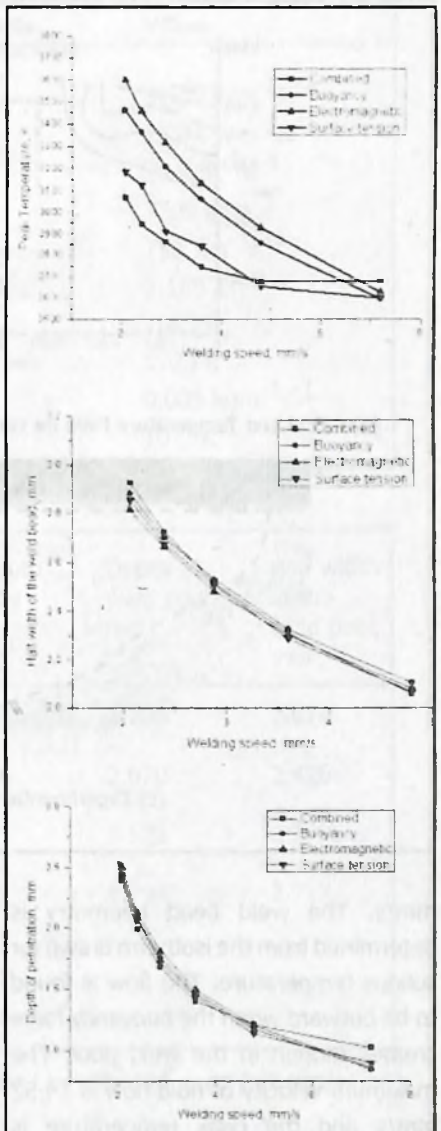

Fig. 4 : Effect of heat input on theoretically calculated peak temperature, weld bead half width and depth of penetration

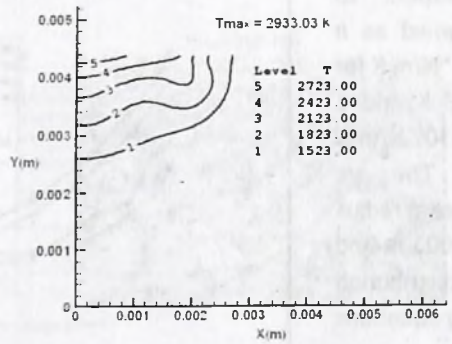

(a) Calculated Temperature Field for combined driving forces

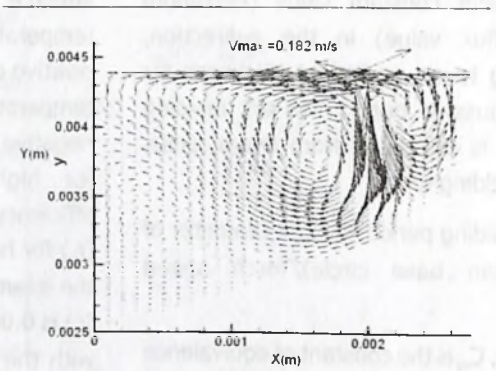

(b) Calculated Velocity Field for combined driving forces

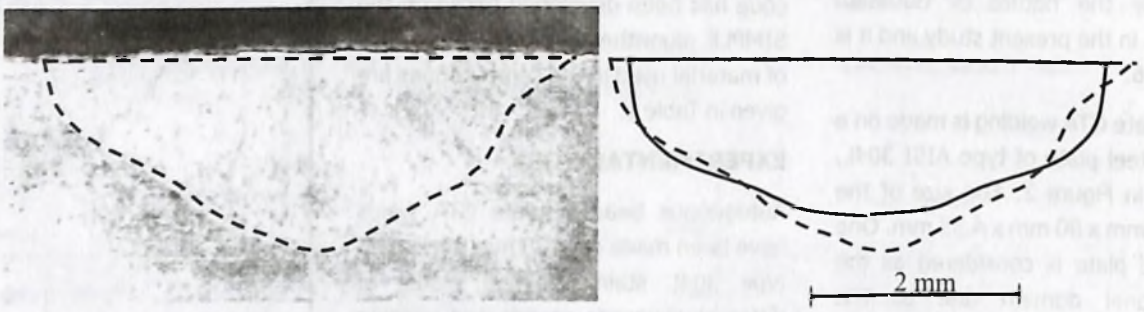

(c) Experimental weld bead (Macrograph) and comparison with theoretical weld bead

Fig. 5 : Results of welding at 120 A at 2.66 mm/s

mm/s. The weld bead geometry is determined from the isotherm drawn for solidus temperature. The flow is found to be outward when the buoyancy force creates motion in the weld pool. The maximum velocity of fluid flow is 14.52 mm/s and the peak temperature is 3101.32 K. The weld bead half width and depth are 2.674 mm and 1.7 mm respectively.

The fluid flow takes place inward when the electromagnetic force alone is acting on the molten metal. The peak temperature in the weld pool is more than that of buoyancy flow. The fact is that in the buoyancy fluid flow, the heat is taken away from the center of the weld pool to outside whereas in the case of convection due to electromagnetic force, the fluid is moved from outside to the center of the weld pool, resisting the heat flow from the center of the weld pool to outside. This leads to the increased depth of penetration and reduced width of the weld bead. The maximum velocity is 28.5922 mm/s and the peak temperature in the weld pool is 3225.06 K. The weld bead half width and depth are 2.426 mm and 2.07 mm respectively.

The maximum fluid velocity in the weld pool is calculated as 167.202 mm/s when the surface tension force alone is acting in the weld pool. The fluid flow is in the inward direction until the temperature reaches 2200 K for stainless steel having 80 ppm sulphur content. A double loop circulation is found as the temperature exceeds 2200 K. The outward flow takes place in the region (center of the weld pool) where the temperature is more than 2200 K and inward flow takes place outside the weld pool where the temperature is below 2200 K. The heat dissipation from the weld pool is comparatively high as the magnitude of velocity of fluid flow is high for surface tension induced flow. Hence, the peak temperature in the weld pool is reasonably low. The peak temperature is calculated as 2687.72 K. The weld bead half width and depth measure 2.7795 mm and 1.523 mm respectively.

The effect of welding speed (heat input) at a particular welding current and voltage on peak temperature in the weld pool and weld bead geometry is shown in Figure 4. The peak temperature, half width of weld bead and depth of penetration increase with heat input (decrease with welding speed), irrespective of the driving force acting on the weld pool. The rate of increase in the peak temperature is high for electro magnetic and buoyancy driven flows. The higher range of fluid velocity in both surface tension driven flow and combined driving forces driven flow, results in lower peak temperature. Hence, the rate of increase in the peak temperature for these two cases is low. Higher weld bead width is calculated for

buoyancy and combined driving forces and deeper penetration is calculated for electromagnetic forces. The combined driving forces driven flow has comparatively maximum width at lower welding speed and maximum penetration at higher welding speed.

Figure 5 shows the calculated temperature and velocity fields for the combined buoyancy, electromagnetic and surface tension forces and the comparison between experimental and theoretical weld bead geometries for the welding condition of 120 A, 14 V and 2.66 mm/s. Table 3 presents the comparison of theoretical results for combined driving forces and the experimental results for two different welding speed at 120 A and 14 V.

CONCLUSIONS

The temperature and velocity fields in the weld pool have been determined using the numerical model based on finite volume method. The effect of individual driving forces has been studied in detail. This work clearly indicates the two dimensional heat and fluid flow model with modified Gaussian heat distribution for heat flux predicts the temperature and velocity fields and bead geometry. The predicted results for bead geometry compares well with the experimental bead geometry.

Properties	Symbols	Value
Thermal Conductivity(solid)	k_S	31.39 $Wm^{-1}K^{-1}$
Thermal Conductivity(liquid)	k_l	15.48 $Wm^{-1}K^{-1}$
Convection heat transfer coefficient	h	20 $Wm^{-2}K^{-1}$
Density	?	7200 kgm^{-3}
Specific Heat	C_p	753 $Jkg^{-1}K^{-1}$
Latent Heat	?H	2.1E9 Jm^{-3}
Solidus Temperature	T_{sol}	1523 K
Liquidus Temperature	Tllq	1723 K
Viscosity	μ	0.005 $kgm^{-1}s^{-1}$
Coefficient of thermal expansion	ß	10^{-4} K^{-1}

Table 1 : Properties of AISI 304L stainless steel

Driving Force	Peak Temperature, K	Maximum Velocity m/s	Depth of weld pool, mm	Half width of the weld pool, mm
Buoyancy	3101.32	0.0145	1.700	2.674
Electromagnetic	3225.06	0.0286	2.070	2.426
Surface tension	2687.72	0.167	1.523	2.7795
Combined Buoyancy, Electromagnetic and Surface tension	2933.03	0.182	1.793	2.717

Table 2 : Theoretical results of GTA welding of SS 304 L at 120 A, 14 V and 2.66 mm/s

REFERENCES

1. D. Rosenthal, Mathematical theory of heat distribution during welding and cutting. Welding Journal, 20-5(1941), 220-s - 234-s.
2. G.M.Oreper, T.W.Eagar, J.Szekely, Heat and fluid flow phenomena in weld pools. Journal of fluid mechanics, 147 (1984) 53 79.
3. T. Zacharia, A.H. Eraslan, D.K.Aidun, Modeling of autogenous welding. Welding Journal, 67 (1988), 53-s - 63-s.
4. M.C.Tsai, S.Kou, Marangoni convection in weld pools with a free surface. International Journal for Numerical Methods in Fluids, 9 (1989)1503- 1516.
5. M.C.Tsai and S.Kou, Electro-magnetic force induced convection in weld pools with a free surface. Welding Journal, 69 (1990) 241-s 246-s.

Table 3 : Comparison of theoretical and experimental results

Run No.	Current, Ampere	Voltage, Volt	Speed mm/s	Heat input, kJ/mm	Theoretical bead dimension, mm Depth	Theoretical bead dimension, mm Width	Experimental bead dimension, mm Depth	Experimental bead dimension, mm Width
1.	120	14.0	5.00	0.336	1.098	4.213	1.150	4.01
2.	120	14.0	2.66	0.630	1.793	5.434	2.100	5.53